Original Article

A novel neoadjuvant therapy for early-stage non-small cell lung cancer in a mouse model

Lanlin Zhang[1], Jiangyuan Du[2], Xianghua Wu[3]

[1]Department of Medical Oncology, Tongji Hospital, School of Medicine, Tongji University, Shanghai, China; [2]Laboratory for Reproductive Immunology, Hospital of Obstetrics and Gynecology, Fudan University Shanghai Medical College, Shanghai, China; [3]Department of Medical Oncology, Fudan University Shanghai Cancer Center, Shanghai, China

Contributions: (I) Conception and design: L Zhang, X Wu; (II) Administrative support: J Du; (III) Provision of study materials or patients: L Zhang, J Du; (IV) Collection and assembly of data: L Zhang, J Du; (V) Data analysis and interpretation: L Zhang, X Wu; (VI) Manuscript writing: All authors; (VII) Final approval of manuscript: All authors.

Correspondence to: Xianghua Wu, MD. Department of Medical Oncology, Fudan University Shanghai Cancer Center, 270 Dong'an Road, Xuhui District, Shanghai 200032, China. Email: xianghua_wu@fudan.edu.cn.

Background: Lung cancer is the common malignancy with high mortality rate in the world. Even with curative resection for early-stage lung cancer patients, the rate of postoperative recurrence and metastasis is still high. Neoadjuvant nivolumab combined with chemotherapy leads to improved pathological complete response rate and event-free survival in resectable non-small cell lung cancer (NSCLC) patients. However, the neoadjuvant therapy is not only accompanied by grade 3 or above adverse events which resulting in the potential missing out on the window for curative surgery for the patients, but also has low efficacy especially in patients with low programmed death ligand 1 (PD-L1) expression. Hence, it is particularly important to explore innovative ways to inhibit tumour recurrence and metastasis.

Methods: In the present study, we investigated whether neoadjuvant therapy with intralesional Rose Bengal (RB) elicited specific immune responses compared with control group, and then the lung cancer mouse model was used to evaluated the immunological mechanism.

Results: The secondary Lewis lung cancer cells (LLCs) tumour growth was significantly suppressed by RB intralesional injection into subcutaneous tumour; the formation rate of secondary tumours induced by the B16 melanoma cell injection was 100%. Intralesional RB neoadjuvant therapy before surgical resection exhibited effectively enhanced T central memory cells (Tcm) and T memory stem cells (Tscm) + naïve T cells (Tn) infiltration, elicited stronger cytotoxic T lymphocyte (CTL) responses against LLCs, and displayed markedly higher proportions of splenic lymphocytes that produce tumour necrosis factor-alpha (TNF-α) and interferon-gamma (IFN-γ) upon restimulation in a lung cancer mouse model.

Conclusions: Based on our preclinical data, neoadjuvant therapy with intralesional RB injection generated immune memory and prevented the recurrence and metastasis of tumour in a lung cancer mouse model, which provides a new strategy for neoadjuvant treatment of early-stage NSCLC.

Keywords: Neoadjuvant therapy; Rose Bengal (RB); immune memory; tumour recurrence

Submitted Oct 06, 2023. Accepted for publication Dec 29, 2023. Published online Feb 23 2024.
doi: 10.21037/jtd-23-1555
View this article at: https://dx.doi.org/10.21037/jtd-23-1555

Introduction

Background

Lung cancer is the common malignancy with high mortality rate in the word, and 46% of lung cancer patients are already in the middle and late stages at the time of initial diagnosis, with a 5-year relative survival rate of only 22% (1). Surgery is the preferred treatment for early-stage lung cancer patients, and even with curative resection, the rate of postoperative recurrence and metastasis is still as high as 30% to 55% (2), and the local recurrence rate is 19%, even for patients in stage IA (3). To date, neoadjuvant chemotherapy combined with immune-checkpoint inhibitors targeting programmed cell death protein 1 (PD-1) or programmed death ligand 1 (PD-L1) for nonmetastatic lung cancer has significantly reduced systemic recurrence and improved long-term overall survival (OS) or cure rates in resectable non-small cell lung cancer (NSCLC) patients (4). CheckMate-816 first showed that compared with chemotherapy alone, neoadjuvant nivolumab combined with chemotherapy leads to improved pathological complete response rate and event-free survival in resectable NSCLC patients (5). However, the neoadjuvant therapy is not only accompanied by grade 3 or above adverse events which resulting in the potential missing out on the window of curative surgery for the patients, but also has low efficacy especially in patients with low PD-L1 expression (6-8).

Photosensitizer-based photodynamic therapy (PDT) has emerged as a promising cancer therapy due to its efficiency in triggering immunogenic cell death (ICD) (9). ICD can be characterized by damage-associated molecular patterns (DAMPs), such as calreticulin (CRT), high-mobility group box 1 protein (HMGB1), and adenosine triphosphate (ATP), which are exposed or secreted by dying cells and act as "eat me" and "danger" signals for the immune system by inducing antigen-presenting cell (APC) activation, antigen processing and T-cell activation (10,11). Moreover, cancer cells undergoing ICD also generate tumour-associated antigens (TAAs) and proinflammatory cytokines after tumour PDT, that can stimulate and amplify tumour-specific immune responses to reinforce antitumour effects (9,12). Some photosensitizers, such as Rose Bengal (RB) or hypericin, have been shown to enhance the responses to antitumour immunization (13). In particular, our published research on RB, which has few side effects on normal cells (14), has confirmed that an *in situ* intralesional RB and immature dendritic cells (DCs) vaccine not only destroys the primary tumour but also prevents tumour relapse by specific antitumour immunity (14). A phase II clinical study in melanoma found that an intratumoural injection of RB could eliminate the uninjected tumour tissue through the bystander effect in addition to effectively killing the primary tumour (15). Moreover, a long-term antitumour immune response was also found in 50% of patients in a study on intratumoural RB treatment in human liver cancer (16). Based on its effectiveness in treating tumours, RB gets the permission for clinical application by the Food and Drug Administration (FDA).

To date, strategies to reduce the recurrence and metastasis of early- to mid-stage NSCLC are very limited. While neoadjuvant therapy for resectable NSCLC has become the default treatment, quite a few questions remain unresolved, such as how to reverse immunosuppressive microenvironments and improve antitumour responses *in situ* (8). Moreover, it is difficult to ensure that these neoadjuvant treatments can generate a long-term antitumour immune response to eradicate minimal residual disease (MRD) and further inhibit tumour recurrence (17). Our previous publication found that the RB-immature DC vaccine could effectively deter tumour recurrence and metastasis by inducing a long-term memory response in a lung cancer mouse model (14), but there are no studies on whether intralesional RB could induce immune memory in early-stage lung cancer patients before surgical resection. Hence, we hypothesized that, as an innovative therapy, intralesional RB neoadjuvant therapy for NSCLC can

Highlight box

Key findings

- This manuscript showed a novel neoadjuvant therapy with intralesional Rose Bengal (RB) injection for early-stage non-small cell lung cancer (NSCLC) in a mouse model.

What is known and what is new?

- Neoadjuvant therapy is not only accompanied by grade 3 or above adverse events which result in a patient the potential missing out on the window for curative surgery, but also has low efficacy especially in programmed death ligand 1 negative patients, even though it improves event-free survival and pathological complete response rates.
- This manuscript explored an innovative way with intralesional RB combined with surgery to inhibit tumour recurrence and metastasis in a mouse model.

What is the implication, and what should change now?

- This manuscript provides a new strategy for neoadjuvant treatment of early-stage NSCLC.

generate a durable immune response before surgical resection, thereby inhibiting tumour recurrence and metastasis and improving the 5-year survival rate of early-stage NSCLC patients. We present this article in accordance with the ARRIVE reporting checklist (available at https://jtd.amegroups.com/article/view/10.21037/jtd-23-1555/rc).

Methods

Cell lines

The Lewis lung cancer cell (LLC) line and the murine melanoma B16 cell line were cultured according to American Type Culture Collection (AJCC) guidelines and were maintained in Dulbecco's modified Eagle medium (DMEM; Gibco, Crand Island, NY, USA; 10569010) and RPMI-1640 medium (Gibco; 61870044) with 10% fetal bovine serum (FBS; Biological Industries, Kibbutz Beit Haemek, Israel; 04-007-1A), penicillin (100 U/mL), and streptomycin (100 µg/mL). All cells were cultured at 37 ℃ in an incubator with 5% CO_2.

Antibodies and reagents

The following antibodies were used in this study: FITC-conjugated anti-CD3e (145-2C11); Brilliant Violet 510™-conjugatedanti-CD8-alpha (53-6.7); purified anti-CD16/CD32 (2.4G2); phycoerythrin (PE)-conjugated anti-CD44 (IM7); PE-Cy7™-conjugatedanti-CD62L (MEL-14); Brilliant Violet 421™-conjugated anti-interferon-gamma (IFN-γ; XMG1.2); and Brilliant Violet 421™-conjugated anti-tumour necrosis factor-alpha (TNF-α; MP6-XT22). RB [330,000] and all of other chemicals were sold by the Sigma-Aldrich Company (Darmstadt, Germanty).

Flow cytometry

A Beckman Coulter Cytomics FC500 Flow Cytometry System was used for flow cytometric analysis. The results were analysed by CXP and FlowJo v10 software.

In vivo tumour protection experiments

Animal experiments were performed in Fudan University Experimental Animal Center (Shanghai, China). All animal experimental protocols were permitted by the Institutional Animal Care and Use Committee of Fudan University, and the agreement number is 20171143A083, in compliance with institutional guidelines for the care and use of animals. Male C57BL/6 mice (aged 6–8 weeks) were sold by Shanghai Lingchang BioTech Co., Ltd. (Shanghai, China).

To establish the subcutaneous xenograft mouse model (n=6 per group), 1×10^6 LLCs were subcutaneously injected into the right flank of C57BL/6 mice. When the tumour diameter was 4–5 mm, the tumours that were treated for 24 h were resected on day 0, and then the development of immunological memory in the mice was tested within 2 weeks by using a rechallenge with LLCs and syngeneic B16 melanoma cells on day 12. Three test groups were designed: (I) RB resection: when the tumour diameter was 4–5 mm, the tumour was injected with 1 mM RB at an injection volume equal to two-thirds of the tumour volume, and the primary tumour was completely removed after 24 h; (II) phosphate buffered saline (PBS) resection: when the tumour diameter was 4–5 mm, the primary tumour was injected with PBS at an injection volume equal to two-thirds of the volume of the tumour, and then the tumour was completely removed after 24 h; and (III) RB no resection: when the tumour diameter was 4–5 mm, the primary tumour was injected with 1 mM RB at an injection volume equal to two-thirds of the volume of the tumour, but the tumour was not removed. The formation of immune memory cells occurs within 1 to 2 weeks (18), so after 12 days, 1×10^6 LLCs and 1×10^6 B16 cells were injected into the right and left hind thighs of the mice, respectively. On day 21, the mouse tumours were observed.

Protocol of single spleen lymphocyte cell suspension

Single-cell suspensions were isolated from the spleen after the mechanical dissociation and enzymatic digestion. First, the spleen was obtained aseptically, minced into 1–2 mm^3 pieces, then washed by RPMI-1640 medium. Tumour tissue was digested by constant shaking for 20 min at room temperature in PBS containing 1 mg/mL collagenase D and 30 µg/mL DNase I. The 70 µm nylon mesh filter was used to remove any undigested tissue fragments from the cell suspension, and the density gradient centrifugation was used to isolate the lymphocytes. Lymphocytes were then washed twice in RPMI-1640 medium and stained with the following antibodies to determine the proportions of T effector memory cells (Tem), T central memory cells (Tcm), T memory stem cells (Tscm), and naïve T cells (Tn) according to the manufacturer's instructions. Tcm were

identified as $CD8^+CD44^+CD62L^+$ cells, Tem were identified as $CD8^+CD44^+CD62L^-$ cells, and Tscm + Tn were identified as $CD8^+CD44^-CD62L^+$ cells. The cells were then washed by flow buffer (PBS with 2% FBS) and resuspended in DNA staining solution [1 μg/mL 4',6-diamidino-2-phenylindole (DAPI)] with 500 μL volume at room temperature for 5 min. The immune cells were analysed by flow cytometry.

Cytotoxicity assay in vitro

The CytoTox 96®Non-Radioactive Cytotoxicity Assay (Promega, Madison, WI, USA; G1780) was used to assess the splenic lymphocyte cytotoxicity according to the manufacturer's instruction. The spleen of each of the mouse was harvested at the end of the experiment. Splenic lymphocytes were stimulated with LLCs that treated with 1 mM RB (RB-treated LLCs) for 5 days and then used as the effector cells. While the targeted cells were LLCs and B16s. Briefly, 8×10^3 LLCs were cultured in one well of 96-well round-bottom plate. The effector splenic lymphocytes were distributed in triplicate wells, and the effector cells were mixed with the target cells (LLCs and B16s) and the effector/target cells (E:T) ratios were 25:1, 12:1, 6:1, and 3:1 in 100 μL final volume. All effector and target cells were centrifuged after 6 h incubation at 37 ℃ in 96-well round-bottom plates. To determine the maximum release, 10 μL of 10× lysis buffer was added to the positive control wells and incubated for 45 min at 37 ℃ before the centrifugation. Then, 50 μL suspension was carefully transferred to a new 96-well round-bottom plate and each well was added 50 μL substrate, then mixed and incubated for 30 min in the dark at room temperature. Finally, each well was pipetted 50 μL stop solution. The plate was read at 490 nm, and the specific lysis percentage in each well was calculated by the following equation: % cytotoxicity = 100 × (experiment – effector spontaneous – target spontaneous)/(target maximum – target spontaneous).

Cytokine generation in vitro

Cytokines produced by antigen-specific $CD8^+$ T cells *in vitro* were evaluated by the following protocol. The spleen of each mouse was harvested at the end of the experiment. Then single spleen lymphocyte cells were obtained according to the protocol above (protocol of single spleen lymphocyte cell suspension). Then, the splenic lymphocytes (2×10^6) of the PBS resection, RB resection, and RB no resection groups were incubated with RB (1 mM)-treated LLCs. After 2 h restimulation, 2 μM brefeldin A and 3 μg/mL monensin (both from eBioscience, Carlsbad, CA, USA) were treated for 4 h, and then all samples were resuspended in 50 μL cocktail composed of diluted antibodies against cell surface markers and incubated for 30 min at 4 ℃. To stain intracellular TNF-α and IFN-γ, 100 μL fixation buffer (eBioscience) was added to the cells suspended in 100 μL staining buffer and incubated for 30 min at 4 ℃. After washing twice in 1× permeabilization buffer, the cells were resuspended in diluted intracellular antibody cocktail, incubated for 30 min at 4 ℃, and then washed twice in 1× permeabilization buffer again. Flow cytometry data were then collected and analysed. A protocol was prepared before the study without registration.

Statistical analysis

GraphPad Prism 5 (GraphPad Software Inc., La Jolla, CA, USA) were performed to all statistical analyses. One-way analysis of variance (ANOVA) followed by the appropriate *post-hoc* test (Tukey's multiple comparison test) and Student's *t*-test were used to compare the differences among individual data points. $P<0.05$ was considered a statistically significant difference.

Results

Experimental design of protective immune response in a lung cancer mouse model

To examine whether intralesional RB followed by curative surgery triggered a specific immune response in an *in vivo* model system, we investigated whether the primary tumour treated by intralesional RB could inhibit the growth of a secondary tumour in mice. The primary tumour was surgically removed 24 h after PBS or RB treatment. The ability of the mice to form an immunological memory response within 2 weeks was tested by rechallenge with LLCs and syngeneic B16 melanoma cells on day 12. The tumour cells (1×10^6 cells per mouse) were inoculated 9 days after the primary tumour was removed to investigate whether immunological memory formed in mice (*Figure 1A*). The timeline for the surgical removal of the primary tumour after PBS or RB treatment was presented in *Figure 1B*.

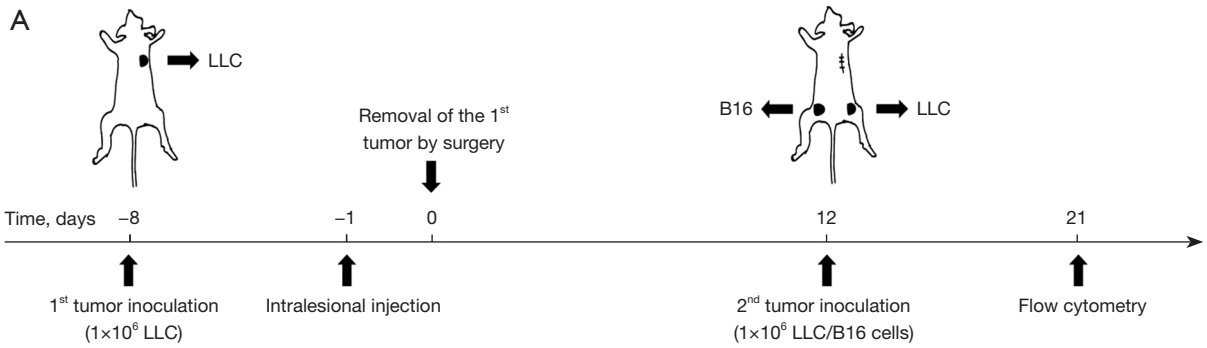

B

	intralesional injection	Removal of the 1st tumor by surgery
PBS resection	PBS	Resection
RB resection	RB	Resection
RB no resection	RB	No resection

Figure 1 Schedules of neoadjuvant therapy. (A) Schematic of the surgical removal of the primary tumour after intralesional PBS or RB to stimulate specific immune responses against the growth of secondary tumours in a subcutaneous tumour model. (B) Three test groups were designed: (I) PBS resection: intralesional PBS injection followed by tumour resection; (II) RB resection: intralesional RB injection followed by tumour resection; and (III) RB no resection: intralesional RB injection without tumour resection. LLC, Lewis lung cancer cell; PBS, phosphate buffered saline; RB, Rose Bengal.

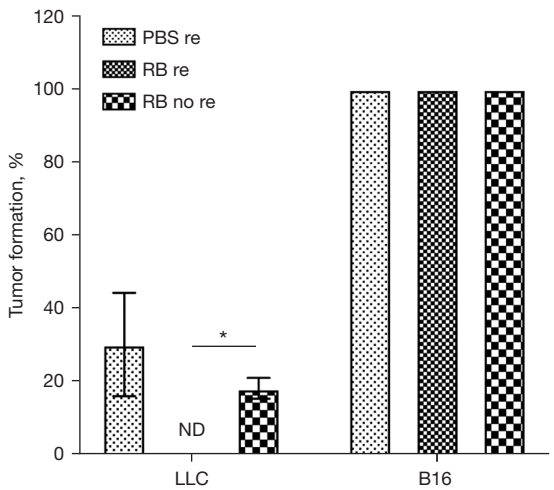

Figure 2 Each group was subcutaneous injected with tumour cells. The formation rate of LLCs and B16 tumours in C57BL/6 mice indicated the number of tumour-forming mice among the total number of mice in each group. The data were representative of three independent experiments. The mean ± SD were shown and the one-way ANOVA was performed, while the significance level was defined as *, P<0.05. PBS, phosphate buffered saline; re, resection; RB, Rose Bengal; LLC, Lewis lung cancer cell; ND, not detected; SD, standard deviation; ANOVA, analysis of variance.

The formation rate of secondary tumours in a lung cancer mouse model

We found that the formation rate of secondary tumours induced by the B16 melanoma cell injection was 100%; the secondary LLC tumour growth in the RB resection group was significantly suppressed compared with that in the PBS resection group and the RB no resection group, and no secondary tumour was observed. In addition, compared with that in the PBS resection group, the secondary LLC tumour formation rate in the RB no resection group was lower (*Figure 2*).

The percentages of memory T cells

The percentages of Tcm from the RB resection and RB no resection groups were much higher than those from the PBS resection group. In contrast, Tem populations were lower in the first two groups. Moreover, Tscm + Tn have been considered to share stem cell-like properties and self-renewal ability upon antigen recounter (19,20), and their proportions in the RB resection group and RB no resection group were markedly increased compared with those of the PBS resection group (*Figure 3A,3B*).

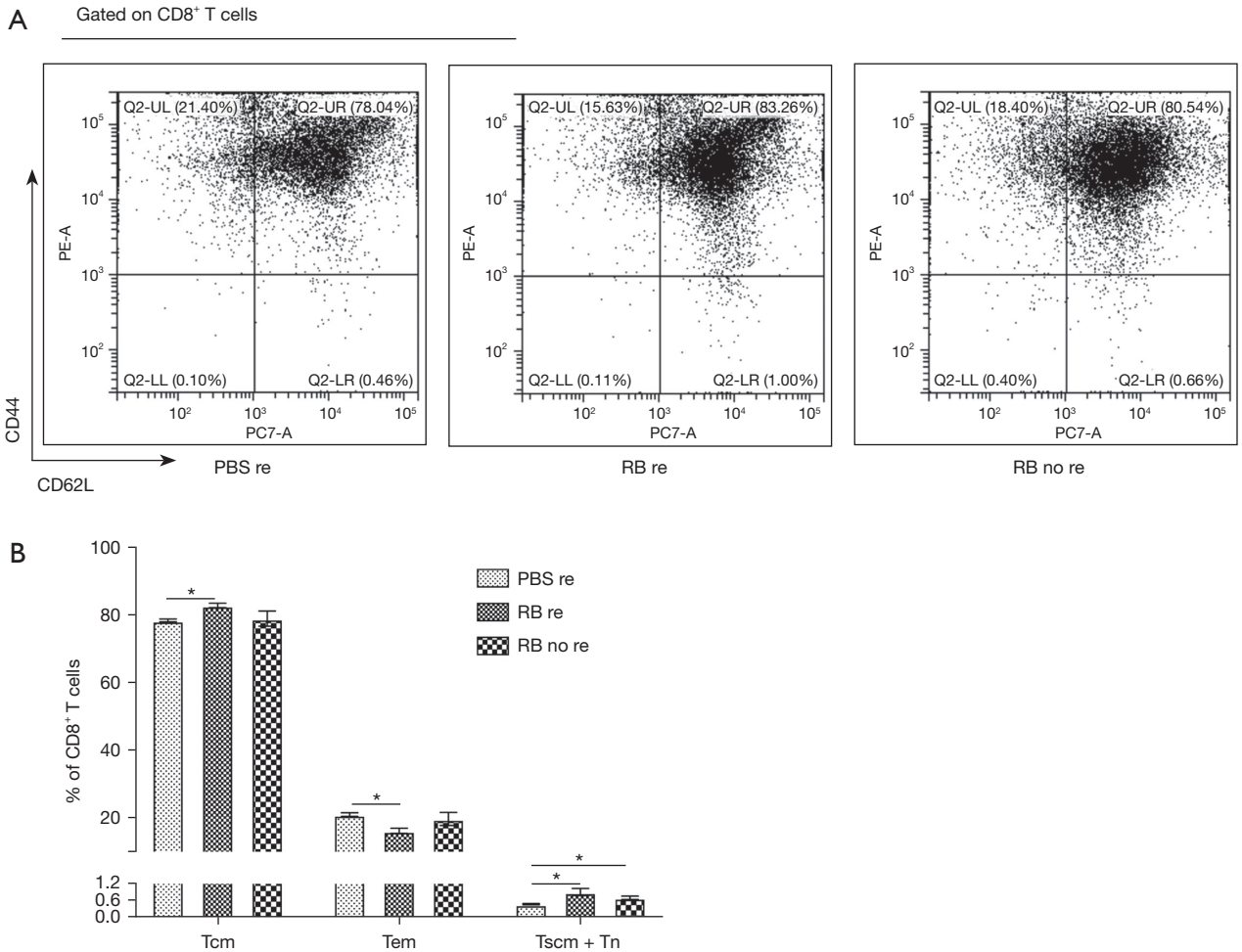

Figure 3 The percentages of $CD62L^{-}CD44^{+}$, $CD62L^{+}CD44^{-}$, and $CD62L^{+}CD44^{+}$ cells among the total $CD8^{+}$ T-cell population. (A) CD8, CD44, and CD62L were used to analyze T-cell. Different types of $CD8^{+}$ T cells were gated individually. Tcm, Tem, and Tscm + Tn were separately identified as $CD8^{+}CD44^{+}CD62L^{+}$, $CD8^{+}CD44^{+}CD62L^{-}$, or $CD8^{+}CD44^{-}CD62L^{+}$. Representative flow cytometric analysis of Tem, Tcm, and Tscm + Tn in the spleens of mice in different group was shown. Representative example of three separate experiments was summarized in (B). The mean ± SD were shown and one-way ANOVA was performed, while the significance level was defined as *, $P<0.05$. PBS, phosphate buffered saline; re, resection; RB, Rose Bengal; Tcm, T central memory cells; Tem, T effector memory cells; Tscm, T memory stem cells; Tn, naïve T cells; SD, standard deviation; ANOVA, analysis of variance.

Cytotoxic T lymphocyte (CTL) activity of mouse splenic lymphocytes

To evaluate whether the RB resection group was superior to the PBS resection group and the RB no resection group in inducing specific CTL responses to LLC and B16 cells *in vivo*, we analysed the CTL activity of the mouse splenic lymphocytes from the mice in the RB resection, PBS resection and RB no resection groups via the CytoTox 96® Non-Radioactive Cytotoxicity Assay. Compared to the other two groups, the RB resection group was capable of eliciting the strongest CTL responses against LLC cells. However, the RB resection group did not exhibit CTL responses against B16 cells, which was consistent with the results for the other groups (*Figure 4A-4C*). At an E:T ratio of 25:1, the CTL activities from the mice in RB resection, PBS resection and RB no resection groups all triggered significantly higher CTL responses against tumour-specific LLC cells.

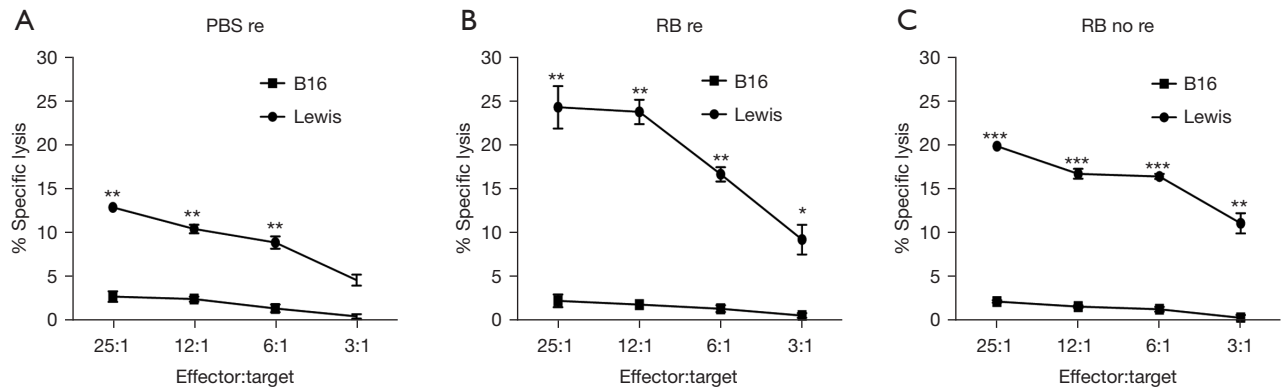

Figure 4 CTL responses in the mice from the PBS resection group (A), RB resection group (B), and RB no resection group (C). CTL responses *in vitro* were assessed with the target cells of LLCs/B16 cells and the effector cells of splenic lymphocytes stimulated with RB-treated LLCs. The representative data of three independent experiments were shown. The mean ± SD were shown. Student's *t*-test was performed, and the significance level was defined as *, P<0.05; **, P<0.01; and ***, P<0.01. PBS, phosphate buffered saline; re, resection; RB, Rose Bengal; CTL, cytotoxic T lymphocyte; LLC, Lewis lung cancer cell; SD, standard deviation.

The proportions of TNF-α- and IFN-γ-producing splenic lymphocytes

The mice from the RB resection group displayed markedly higher proportions of TNF-α- and IFN-γ-producing splenic lymphocytes upon restimulation than the mice from the other two groups (*Figures 5A*,*5B*,*6A*,*6B*). There was no significant difference between the PBS resection and RB no resection groups.

Discussion

In the present study, we found that the secondary LLC tumour growth in the RB resection group was significantly suppressed compared with that in the control group. Even though the percentages of Tcm and Tscm + Tn from the RB resection and RB no resection groups were much higher than those from the PBS resection group, the RB resection group was capable of eliciting stronger CTL responses against LLC cells and displayed markedly higher proportions of splenic lymphocytes that produce TNF-α- and IFN-γ.

In accordance with previous research on RB, a phase 2 study of intralesional PV-10, a 10% solution of RB, revealed that PV-10 induced an immunologic response that led to cutaneous bystander metastatic melanoma tumour regression (15). Vaccination with *in vitro* RB-treated colon cancer cells resulted in slower tumour growth following inoculation with colon cancer cells due to a specific antitumour immune response (21). Furthermore, a phase 1 study demonstrated that using PV-10 in the chemoablation of hepatocellular cancer and liver metastasis resulted in a long-term tumour-specific objective response rate of 50% (16). Here, we demonstrated that the secondary LLC tumour growth in the RB resection group was significantly suppressed compared with that in the group of PBS resection and the group of RB no resection; however, a better understanding of the mechanism underlying these findings is necessary for selecting the optimal treatment strategy.

To verify whether an antitumour immune response was generated, we determined the expression of memory T cells. The results showed that the RB resection group exhibited effectively enhanced Tcm and Tscm + Tn infiltration, elicited stronger CTL responses against LLC cells, and displayed markedly higher proportions of splenic lymphocytes producing TNF-α and IFN-γ upon restimulation than the RB no resection group. Therefore, these findings suggested that intralesional RB plus surgical resection induced specific immune responses and long-term immune memory. Although we found that the proportions of Tscm + Tn were not significantly different in the RB resection and RB no resection groups, we also observed that the strength of CTL responses and cytokine production (TNF-α and IFN-γ) in the RB no resection group was markedly lower than in the RB resection group. This result was mainly because Tscm + Tn were a mixed cell population; specifically, the proportion of Tscm was lower in the mixed cell population of the RB no resection group than in the RB

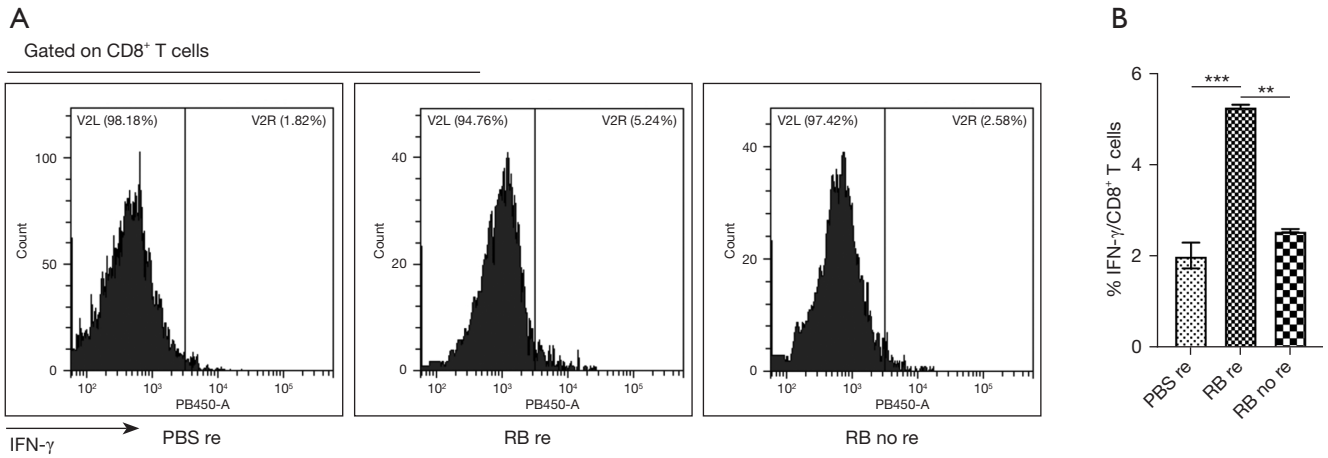

Figure 5 The proportion of IFN-γ-producing splenic lymphocytes. Representative flow cytometric analysis of the percentage of IFN-γ-producing CD8$^+$ T cells among the total CD8$^+$ T-cell population (A). The representative data of three independent experiments were shown (B). The mean ± SD were shown. One-way ANOVA was performed, and the significance level was defined as **, P<0.01; ***, P<0.01. IFN-γ, interferon-gamma; PBS, phosphate buffered saline; re, resection; RB, Rose Bengal; SD, standard deviation; ANOVA, analysis of variance.

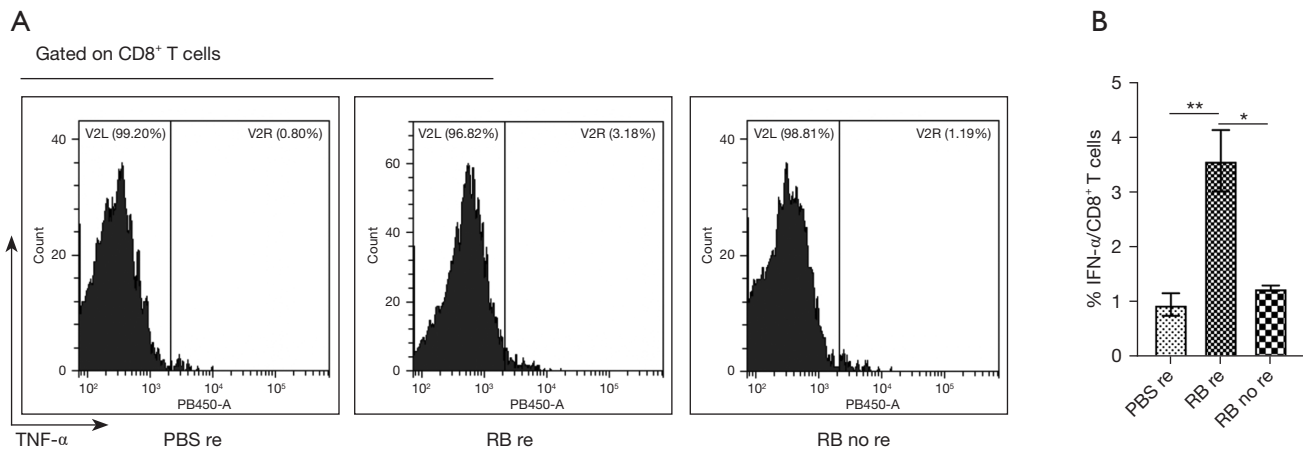

Figure 6 The proportion of TNF-α-producing splenic lymphocytes. Representative flow cytometric analysis of TNF-α-producing CD8$^+$ T cell percentage among the total CD8$^+$ T-cell population (A). The representative data of three independent experiments were shown (B). The mean ± SD were shown. One-way ANOVA was performed, and the significance level was defined as *, P<0.05; **, P<0.01. TNF-α, tumour necrosis factor-alpha; PBS, phosphate buffered saline; re, resection; RB, Rose Bengal; SD, standard deviation; ANOVA, analysis of variance.

resection group. Moreover, persistent antigen stimulation in the RB no resection group could also induce T-cell exhaustion (22). Compared with neoadjuvant nivolumab plus chemotherapy, PDT not only directly kills cancer cells and fully exposes tumour antigens but also induces ICD and triggers antitumour immune responses. This kind of vaccine-like function could be used to transform a "cold" tumour microenvironment into an immunogenic, "hot" tumour microenvironment (23). Therefore, for early-stage tumours with less T-cell exhaustion, neoadjuvant therapy may not need to be combined with immune checkpoint inhibitors, thus reducing adverse events.

Interestingly, we also revealed that the growth of secondary tumours in the mice was partly inhibited by the resection of the primary tumour in the PBS resection group, and this result was associated with the effective antitumour immune responses against tumour-specific transplantation antigens observed during rechallenge (24). This finding

is closely related to the fact that early tumour resection can reduce the depletion of T cells, making more effector T cells become memory T cells (25). Indeed, this finding reaffirms that early tumour resection in NSCLC patients reduces tumour recurrence by 45–70% (26).

Our study did have limitations. For example, the intralesional RB/PBS treatment was not studied at different points. We intratumourally injected RB/PBS into the subcutaneous tumours at approximately 7 days, at which point the tumour diameter was approximately 5 mm. If RB/PBS is intratumourally administered at a tumour diameter of approximately 8 or 10 mm, the high expression of tumour antigens may generate a stronger immune response, and the proportion of Tscm may be different. Future work will further explore this issue.

Conclusions

Based on our preclinical data, the results showed that the secondary LLCs tumour growth was significantly suppressed by RB intralesional injection into subcutaneous tumour in a murine lung cancer model. Intralesional RB neoadjuvant therapy before surgical resection exhibited effectively enhanced Tcm and Tscm + Tn infiltration, elicited stronger CTL responses against LLCs, and displayed significantly higher proportions of splenic lymphocytes that produced TNF-α and IFN-γ upon restimulation. Therefore, this therapeutic approach provides a new strategy for neoadjuvant treatment of early-stage NSCLC.

Acknowledgments

Funding: The study was supported by the Nature Science Foundation of China (grant No. 81372527), the Nature Science Foundation of the Shanghai Municipal Commission of Health and Family Planning (grant No. 201540373), and the Nature Science Foundation of Shanghai (grant No. 12ZR1406500).

Footnote

Reporting Checklist: The authors have completed the ARRIVE reporting checklist. Available at https://jtd.amegroups.com/article/view/10.21037/jtd-23-1555/rc

Data Sharing Statement: Available at https://jtd.amegroups.com/article/view/10.21037/jtd-23-1555/dss

Peer Review File: Available at https://jtd.amegroups.com/article/view/10.21037/jtd-23-1555/prf

Conflicts of Interest: All authors have completed the ICMJE uniform disclosure form (available at https://jtd.amegroups.com/article/view/10.21037/jtd-23-1555/coif). The authors have no conflicts of interest to declare.

Ethical Statement: The authors are accountable for all aspects of the work in ensuring that questions related to the accuracy or integrity of any part of the work are appropriately investigated and resolved. Experiments were performed under a project license (No. 20171143A083) granted by the Institutional Animal Care and Use Committee of Fudan University, in compliance with institutional guidelines for the care and use of animals.

References

1. Siegel RL, Miller KD, Fuchs HE, et al. Cancer statistics, 2022. CA Cancer J Clin 2022;72:7-33.
2. Uramoto H, Tanaka F. Recurrence after surgery in patients with NSCLC. Transl Lung Cancer Res 2014;3:242-9.
3. Fedor D, Johnson WR, Singhal S. Local recurrence following lung cancer surgery: incidence, risk factors, and outcomes. Surg Oncol 2013;22:156-61.
4. Kang J, Zhang C, Zhong WZ. Neoadjuvant immunotherapy for non-small cell lung cancer: State of the art. Cancer Commun (Lond) 2021;41:287-302.
5. Leal TA, Ramalingam SS. Neoadjuvant therapy gains FDA approval in non-small cell lung cancer. Cell Rep Med 2022;3:100691.
6. Provencio M, Nadal E, Insa A, et al. Neoadjuvant chemotherapy and nivolumab in resectable non-small-cell lung cancer (NADIM): an open-label, multicentre, single-arm, phase 2 trial. Lancet Oncol 2020;21:1413-22.
7. Forde PM, Spicer J, Lu S, et al. Neoadjuvant Nivolumab plus Chemotherapy in Resectable Lung Cancer. N Engl J

Med 2022;386:1973-85.
8. Saw SPL, Ong BH, Chua KLM, et al. Revisiting neoadjuvant therapy in non-small-cell lung cancer. Lancet Oncol 2021;22:e501-16.
9. Li X, Lovell JF, Yoon J, et al. Clinical development and potential of photothermal and photodynamic therapies for cancer. Nat Rev Clin Oncol 2020;17:657-74.
10. Fucikova J, Kepp O, Kasikova L, et al. Detection of immunogenic cell death and its relevance for cancer therapy. Cell Death Dis 2020;11:1013.
11. Wiersma VR, Michalak M, Abdullah TM, et al. Mechanisms of Translocation of ER Chaperones to the Cell Surface and Immunomodulatory Roles in Cancer and Autoimmunity. Front Oncol 2015;5:7.
12. Yi Y, Yu M, Li W, et al. Vaccine-like nanomedicine for cancer immunotherapy. J Control Release 2023;355:760-78.
13. Pham TC, Nguyen VN, Choi Y, et al. Recent Strategies to Develop Innovative Photosensitizers for Enhanced Photodynamic Therapy. Chem Rev 2021;121:13454-619.
14. Zhang L, Du J, Song Q, et al. A Novel In Situ Dendritic Cell Vaccine Triggered by Rose Bengal Enhances Adaptive Antitumour Immunity. J Immunol Res 2022;2022:1178874.
15. DePalo DK, Zager JS. Advances in Intralesional Therapy for Locoregionally Advanced and Metastatic Melanoma: Five Years of Progress. Cancers (Basel) 2023;15:1404.
16. Goldfarb P, Low R, Lyon J, et al. P-116 Phase 1 Study of PV-10 for Chemoablation of Hepatocellular Cancer and Cancer Metastatic to the Liver. Ann Oncol 2015;26:iv33.
17. Chae YK, Oh MS. Detection of Minimal Residual Disease Using ctDNA in Lung Cancer: Current Evidence and Future Directions. J Thorac Oncol 2019;14:16-24.
18. Mueller SN, Gebhardt T, Carbone FR, et al. Memory T cell subsets, migration patterns, and tissue residence. Annu Rev Immunol 2013;31:137-61.
19. Sarkar I, Pati S, Dutta A, et al. T-memory cells against cancer: Remembering the enemy. Cell Immunol 2019;338:27-31.
20. Liu Q, Sun Z, Chen L. Memory T cells: strategies for optimizing tumor immunotherapy. Protein Cell 2020;11:549-64.
21. Qin J, Kunda N, Qiao G, et al. Colon cancer cell treatment with rose bengal generates a protective immune response via immunogenic cell death. Cell Death Dis 2017;8:e2584.
22. Li F, Liu H, Zhang D, et al. Metabolic plasticity and regulation of T cell exhaustion. Immunology 2022;167:482-94.
23. Duan X, Chan C, Lin W. Nanoparticle-Mediated Immunogenic Cell Death Enables and Potentiates Cancer Immunotherapy. Angew Chem Int Ed Engl 2019;58:670-80.
24. Peri A, Salomon N, Wolf Y, et al. The landscape of T cell antigens for cancer immunotherapy. Nat Cancer 2023;4:937-54.
25. Chow A, Perica K, Klebanoff CA, et al. Clinical implications of T cell exhaustion for cancer immunotherapy. Nat Rev Clin Oncol 2022;19:775-90.
26. Wang X, Janowczyk A, Zhou Y, et al. Prediction of recurrence in early stage non-small cell lung cancer using computer extracted nuclear features from digital H&E images. Sci Rep 2017;7:13543.

Cite this article as: Zhang L, Du J, Wu X. A novel neoadjuvant therapy for early-stage non-small cell lung cancer in a mouse model. J Thorac Dis 2024;16(2):1108-1117. doi: 10.21037/jtd-23-1555